

C–H···O Hydrogen Bond-Directed Ligand Exchange Reaction: Diastereoselective Synthesis of P,S-Bridged (μ -alkyne)Co₂(CO)₄ Complexes

Jordi Solà,[†] Antoni Riera,^{*,†} Xavier Verdager,^{*,†} and Miguel A. Maestro[‡]

Unitat de Recerca en Síntesi Asimètrica (URSA-PCB), Institute for Research in Biomedicine (IRB), and Departament de Química Orgànica, Universitat de Barcelona, c/Josep Samitier, 1-5, E-08028 Barcelona, Spain, and Departamento de Química Fundamental, Universidade da Coruña, E-15071 A Coruña, Spain

Received July 20, 2006

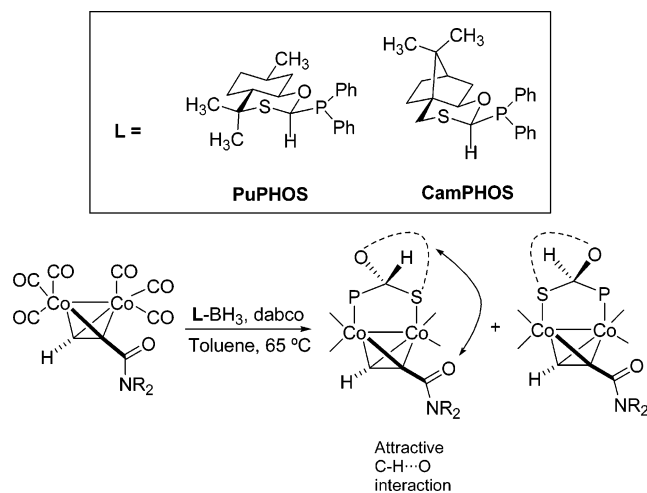
Here we describe a nonclassical interaction between a sulfonyl group in a dicobaltcarbonyl–alkyne complex and a methine moiety attached to three heteroatoms (O, P, S) included in the PuPHOS and CamPHOS ligands. This interaction provides an efficient recognition event that yields up to 86% de in the CO–phosphine exchange reaction. The isomerization mechanism leading to the observed diastereomeric bias was studied computationally at the semiempirical level.

Introduction

Our group has developed the bidentate P,S ligands PuPHOS and CamPHOS (Scheme 1). When coordinated to a terminal alkyne dicobalt complex, these ligands provide two bridged diastereomeric complexes.¹ Upon reaction with norbornadiene, each diastereomer produces the corresponding Pauson–Khand adduct in high optical purity.² Although the utility of these ligands has been demonstrated in the synthesis of chiral cyclopentenones,³ they show poor diastereoselectivity in the ligand exchange process (up to 50% de). To overcome this handicap, we recently reported a hydrogen bond-directed ligand coordination procedure.⁴ The methine moiety attached to three heteroatoms (O, P, S) and contained in PuPHOS and CamPHOS ligands serves as a strong hydrogen bond donor. When an appropriate hydrogen bond acceptor is placed on the alkyne moiety, a nonclassical C–H···O interaction can take place. Given the chirality of the ligand, this interaction can be established only for one of the two possible diastereomers (Scheme 1). Hydrogen bonds are key forces in molecular recognition and are crucial for the stability of biological systems. Nonclassical C–H···X (X = O, N, halogen, π) are important in solvation processes and in biological and supramolecular chemistry.⁵ Nevertheless, applications of weak hydrogen bond interactions in asymmetric synthesis and catalysis are still scarce.⁶

In this scenario, we sought to extend the generality and scope of the directed C–H···O coordination of PuPHOS and Cam-

Scheme 1. Diastereomeric Bridged P, S Complexes in the Presence of an Amidocarbonyl Hydrogen Bond Acceptor



PHOS to weaker hydrogen bond acceptor groups. Here we report on the diastereoselective ligand exchange of P,S ligands with dicobalthexacarbonyl complexes of a sulfonylacetylene. The sulfone group is a weaker hydrogen acceptor than amides and sulfoxides and slightly stronger than ketones and esters.⁷ Thus, the sulfone should help to determine the efficiency of this approach for a variety of widely occurring functional groups.

Results and Discussion

A terminal *p*-tolylsulfonylacetylene dicobalthexacarbonyl complex (**1**) was synthesized following a recently described procedure.⁸ Using the sulfone complex **1** we proceeded to study the ligand exchange reaction with CamPHOS and PuPHOS (Table 1). The reaction was performed by heating a mixture of the corresponding borane-protected phosphine and 1 equiv of **1** at 65 °C in the presence of DABCO (1,4-diazabicyclo[2.2.2]-octane). Thus, borane removal and ligand exchange reaction occurred in a one-pot process.

Ligand exchange reaction of **1** with CamPHOS and PuPHOS provided the corresponding diastereomeric complexes in excel-

* Corresponding author. E-mail: xverdager@pcb.ub.es.

[†] Institute for Research in Biomedicine and Dept. Química Orgànica (UB).

[‡] Universidade da Coruña.

(1) (a) Verdager, X.; Moyano, A.; Pericàs, M. A.; Riera, A.; Maestro, M. A.; Mahia, J. *J. Am. Chem. Soc.* **2000**, *122*, 10242–10243. (b) Verdager, X.; Pericàs, M. A.; Riera, A.; Maestro, M.A.; Mahía, J. *Organometallics* **2003**, *22*, 1868–1877.

(2) For recent reviews on the Pauson–Khand reaction see: (a) Gibson, S. E.; Mainolfi, N. *Angew. Chem., Int. Ed.* **2005**, *44*, 3022–3027. (b) Laschat, S.; Becheanu, A.; Bell, T.; Baro, A. *Synlett* **2005**, *17*, 2547–2570.

(3) (a) Verdager, X.; Lledó, A.; López-Mosquera, C.; Maestro, M. A.; Pericàs, M. A.; Riera, A. *J. Org. Chem.* **2004**, *69*, 8053–8061. (b) Iqbal, M.; Evans, P.; Lledó, A.; Verdager, X.; Pericàs, M. A.; Riera, A.; Loeffler, C.; Sinha, A. K.; Mueller, M. *J. ChemBioChem* **2004**, *6*, 276–280.

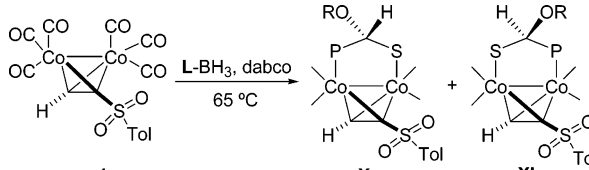
(4) Solà, J.; Riera, A.; Verdager, X.; Maestro, M. A. *J. Am. Chem. Soc.* **2005**, *127*, 13629–13633.

(5) *IUCr Monographs on Crystallography*; Desiraju, G. R., Steiner, T., Eds.; Oxford University Press: New York, 2001; Vol IX.

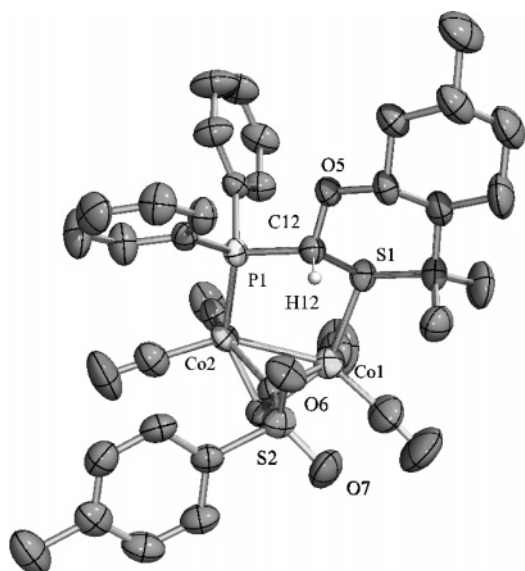
(6) Corey, E. J. *Angew. Chem., Int. Ed.* **2002**, *41*, 1650–1667.

(7) Hunter, C. A. *Angew. Chem., Int. Ed.* **2004**, *43*, 5310–5324.

(8) Solà, J.; Riera, A.; Pericàs, M.A.; Verdager, X.; Maestro, M.A. *Tetrahedron Lett.* **2004**, *45*, 5387–5390.

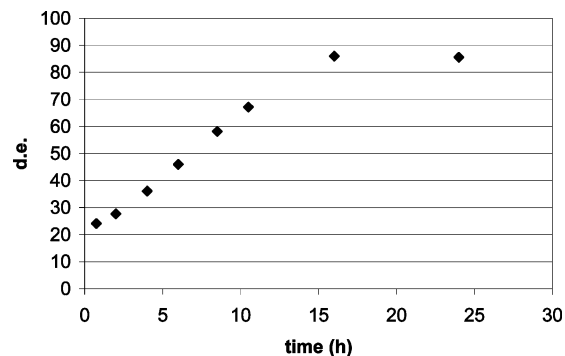
Table 1. Ligand Exchange Reaction for Bidentate P,S Ligands


entry	L	yield (%)	time (h)	Solvent	Xa/Xb	de (%) ^a
1	CamPHOS	96	16	toluene	1a/1b	78
2	PuPHOS	89	16	toluene	2a/2b	86
3	CamPHOS	76	24	hexane	1a/1b	20
4	PuPHOS	88	24	hexane	2a/2b	50
5	CamPHOS	98	16	THF	1a/1b	0
6	PuPHOS	88	16	THF	2a/2b	13

^a As determined by ¹H NMR spectroscopy.**Figure 1.** ORTEP drawing of **2a** with 50% probability ellipsoids. Only the hydrogen providing the weak hydrogen bond is shown.

lent yields as red solids. The best diastereoselectivity was obtained in toluene (Table 1, entries 1 and 2). The reaction in hexane provided lower selectivity than toluene (Table 1, entries 3 and 4), probably because of the reduced product solubility in this solvent even at higher temperatures. Finally, ligand exchange reaction in THF provided no selectivity (Table 1, entries 5 and 6). With respect to the ligand moiety, reactions with PuPHOS were slightly more selective than the corresponding reactions with CamPHOS. These experiments indicate that the C–O···H-directed ligand exchange reaction also occurs when the hydrogen bond acceptor is a sulfone group. The selectivity decreased dramatically when a polar solvent such as THF was used (entries 5, 6). This observation suggests that solvent interference in the weak interaction is responsible for the lower selectivity.

Study of the Weak C–H···O=S Contact. A solid-state study was performed on the major diastereomeric complexes **1a** and **2a**. Fortunately, suitable single crystals of **2a** could be grown layering hexane over toluene. X-ray analysis of **2a** (Figure 1) confirmed that a nonclassical hydrogen bonding was established between the methine (C12, H12) and an oxygen atom from the sulfone group (O6). Bridged ligands show fluxionality around the Co–Co axis.⁹ Dicobalt complexes of terminal

(9) Hanson, B. E.; Mancini, J. S. *Organometallics* **1983**, *2*, 126–128.**Figure 2.** Evolution of diastereomeric excess of complexes **2a/2b** as determined by ¹H NMR analysis.

alkynes bearing a bridged ligand may exist in two fluxional conformations, *anti* and *syn*, depending on the relative position of the alkyne substituent and the bidentate ligand. It is important to note that the hydrogen bond interaction can occur only in the *syn* conformation. For most reported X-ray structures, repulsive steric effects force the ligand to adopt an *anti* conformation away from the alkyne substituent.¹⁰ In the present example, the X-ray structure for **2a** demonstrates that, in the solid state, the weak C–H···O=S bond forces the bidentate ligand and the sulfone group in the alkyne moiety to adopt a *syn* conformation. The distances for C(12)–O(6) and H(12)–O(6) are 3.29(1) and 2.40(1) Å, respectively, and the angles are $\theta(\text{C–H}\cdots\text{O}) = 151.3(5)^\circ$ and $\phi(\text{H}\cdots\text{O–S}) = 112.4(5)^\circ$. These values are consistent with those reported in the literature.¹¹ The H(12)–O(6) distance reported here is larger than that of the amidocarbonyl contact previously described (2.35 Å).⁴

Occurrence of the weak hydrogen bond in solution was confirmed by ¹H NMR in C₆D₆. The methine (H12) resonance for major diastereomers **1a** and **2a** displayed a downfield shift (≈ 0.7 ppm) in comparison with minor diastereomers **1b** and **2b**, which could not provide the stabilizing contact. The interaction energy for the present C–H···O bonding contact was evaluated at the MP2/6311+G(2d,p) level.^{12,13} Single-point calculations on a computing model constructed from the X-ray structure of **2a** yielded an interaction energy of 3.18 kcal/mol.¹⁴ The present estimated energy for the methine–sulfone contact falls in the range of strong C–H···O bonds.

Isomerization of P,S-Bridged (μ -alkyne)Co₂(CO)₄ Complexes. Reaction progress analysis by ¹H NMR indicated that the diastereoselectivity observed in the ligand exchange process is the result of a thermodynamic equilibrium. The selectivity increased to reach, over time, a fixed diastereomeric ratio (Figure 2). Experimentally, the present isomerization process occurs

(10) For X-ray structures of terminal alkyne–dicobalthexacarbonyl complexes with bridged bidentate ligands, see: (a) Gimbert, Y.; Robert, F.; Durif, A.; Averbuch, M.-T.; Kann, N.; Greene, A. E. *J. Org. Chem.* **1999**, *64*, 3492–3497. (b) Verdaguer, X.; Pericàs, M. A.; Riera, A.; Maestro, M. A.; Mahía, J. *Organometallics* **2003**, *22*, 1868–1877.(11) (a) Taylor, R.; Kennard O. *J. Am. Chem. Soc.* **1982**, *104*, 5063–5070. (b) Taylor, R.; Kennard, O. *Acc. Chem. Res.* **1984**, *17*, 320–326. (c) Desiraju, G. R. *Acc. Chem. Res.* **1991**, *24*, 290–296.(12) Corrections for the basis set superposition error (BSSE) were included and were determined through the counterpoise method described by Boys and Bernardi; see: Boys, S. F.; Bernardi, F. *Mol. Phys.* **1970**, *19*, 553–556.(13) Quantum chemical calculations were performed using the Gaussian 03 program package: Frisch, M. J.; et al. *Gaussian 03*, revision C.02; Gaussian, Inc.: Wallingford, CT, 2004.

(14) See Supporting Information for a graphical representation of the computing model.

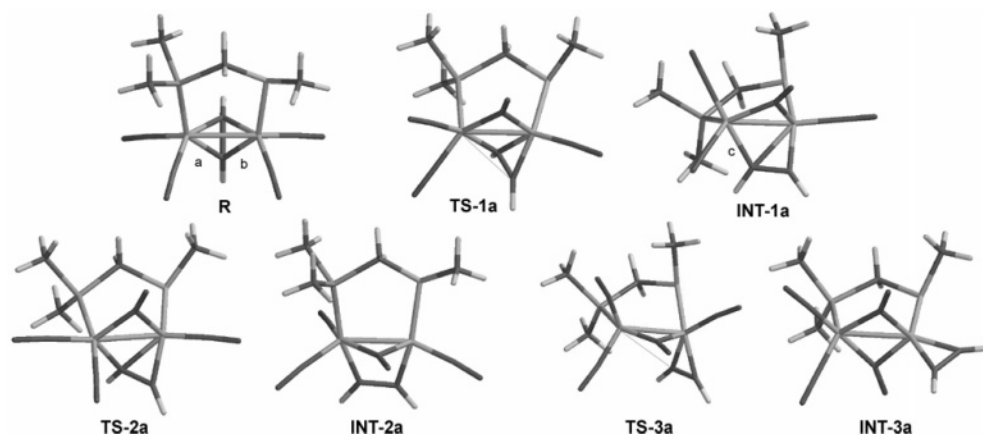


Figure 3. Intermediates and transition states involved in the alkyne-dissociation mechanism for the isomerization of model complex **R**.

under nitrogen in the absence of CO; therefore it is not assisted by external carbon monoxide.¹⁵ Under these conditions, two mechanisms for the interconversion between diastereomeric complexes **Xa** and **Xb** can be envisaged. A first possible isomerization pathway is the equilibration through partial or total dissociation of the alkyne moiety from one of the metal centers. It has been postulated that isomerization of M_2C_2 tetrahedral systems occurs through direct rotation of the alkyne with respect to the metal–metal bond.¹⁶ On the basis of the cluster theory, Jaouen and co-workers proposed a mechanism by which elongation of one of the metal–carbon bonds provides a butterfly-like intermediate.¹⁷ This partial dissociation of the alkyne ligand could evolve to a full dissociation of the alkyne from one cobalt atom¹⁸ or to a formal rotation of the alkyne with respect to the Co–Co axis. An alternative isomerization pathway would imply cleavage of the Co–S bond to form a coordinatively unsaturated complex. Migration of the pendant phosphine would then provide the rearranged complex without the assistance of an incoming CO ligand. This is a reasonable scenario for a P,S ligand such as PuPHOS and CamPHOS, where the sulfur linkage is much weaker than the phosphorus one.¹⁹

To gain further insight into the mechanism of the isomerization process in the absence of CO, we performed a computational study. Geometries of stationary points and transition states (TS) were fully optimized and characterized at the semi-empirical PM3(tm) level, which includes parametrization for transition metals. Reaction pathways were verified by optimization of the perturbed TS structures. Finally, to efficiently compare reaction pathways from the energetic point of view, single-point calculations were performed at the DFT level using the functional B3LYP. For this purpose we used the LACVP* basis set, which includes Hay and Wadt's effective core potential (ECP) for cobalt, while all other atoms are described using a 6-31G* basis set.^{20–22}

(15) Isomerization of phosphine (μ -alkyne) $\text{Co}_2(\text{CO})_5$ complexes is a well-documented process; see: Hay, A.M.; Kerr, W. J.; Kirk, G. G.; Middlemiss, D. *Organometallics* **1995**, *14*, 1986–4988.

(16) Iwashita, Y.; Tamura, F.; Wakmatsu, H. *Bull. Chem. Soc. Jpn.* **1970**, *43*, 1520–1523.

(17) Jaouen, G.; Marinetti, A.; Saillard, J.-Y.; Sayer, B. G.; McGlinchey, M. J. *Organometallics* **1982**, *1*, 225–227.

(18) Partial alkyne dissociation from one metal center was also proposed in the isomerization of $\text{Co}_2(\text{alkyne})(\text{binap})\text{CO}_4$ complexes; see: Gibson, S.E.; Kaufmann, K. A. C.; Loch, J. A.; Steed, J. W.; White, A. J. P. *Chem. Eur. J.* **2005**, *11*, 2566–2576.

(19) For reviews on hemilabile ligands, see: (a) Braunstein, P.; Naud, F. *Angew. Chem., Int. Ed.* **2001**, *40*, 680–699. (b) Dieguez, M.; Pamies, O.; Ruiz, A.; Diaz, Y.; Castillon, S.; Claver, C. *Coord. Chem. Rev.* **2004**, *248*, 2165–2192.

(20) *Spartan '04*; Wavefunction, Inc.; Irvine, CA.

Table 2. Computed Absolute and Relative Energies (DFT) of the Species Involved in the Alkyne-Dissociation Mechanism for the Isomerization of **R**

compound	absolute ΔH_f (au)	relative ΔH_f (kcal/mol)
R	−1719.50628	0.0
TS-1a	−1719.48453	13.6
TS-1b	−1719.48766	11.68
INT-1a	−1719.49333	8.1
INT-1b	−1719.49227	8.8
TS-2a	−1719.47389	20.3
TS-2b	−1719.46910	23.3
INT-2a	−1719.49289	8.4
INT-2b	−1719.48718	11.9
TS-3a	−1719.47200	21.5
INT-3a	−1719.48318	14.5

Using complex **R** as a computing model (Figure 3), we first studied the partial dissociation of the alkyne from one cobalt atom in a butterfly-like mechanism.¹⁷ Starting from **R**, enlargement of bond (a) and concomitant arrangement of a carbonyl ligand in a bridging position allowed the location of **TS-1a**, which subsequently led to a butterfly-like intermediate, **INT-1a**. A pseudosymmetrical reaction pathway was located upon elongation of bond (b) in **R**, which allowed us to locate **TS-1b** and **INT-1b**. Absolute and relative energies for all the intermediates are shown in Table 2. From **INT-1a**, inversion of the cobalt center attached to phosphorus through a pseudo-octahedral transition state (**TS-2a**) led to **INT-2a**, in which the alkyne is arranged along the same plane as the cobalt–cobalt bond. **INT-2a** is a 1,2-dimetallacyclobutene and represents a formal half rotation of the alkyne around the Co–Co axis.¹⁶ From **INT-2a** a symmetrical reaction pathway would provide the isomerized starting material. Alternatively, from **INT-1a** another isomerization pathway involving full dissociation of the alkyne from one of the metal centers was computed. Thus, elongation of bond (c) in **INT-1a** permitted us to locate **TS-3a**. Moving the alkyne moiety further from the departing metal center with the concomitant formation of another bridged carbonyl ligand provided **INT-3a**, in which the alkyne is bonded to only one cobalt atom. The intermediate **INT-3a** would provide free rotation of the alkyne moiety and could also account

(21) PM3(tm) provides a good reproduction of the structural features of X-ray crystal data for alkyne–dicobalt carbonyl complexes. However, this level of theory shows a tendency to saturate vacant coordination sites on cobalt through bridging carbonyls or through agostic interactions with hydrogen atoms. See: Verdaguier, X.; Vazquez, J.; Fuster, G.; Bernardes-Genisson, V.; Greene, A. E.; Moyano, A.; Pericas, M. A.; Riera, A. J. *Org. Chem.* **1998**, *63*, 7037–7052. To validate the significance of intermediates bearing bridging carbonyls, independent geometry optimization of these structures was performed at the DFT level.

(22) Hay, P. J.; Wadt, W. R. *J. Chem. Phys.* **1985**, *82*, 270–283.

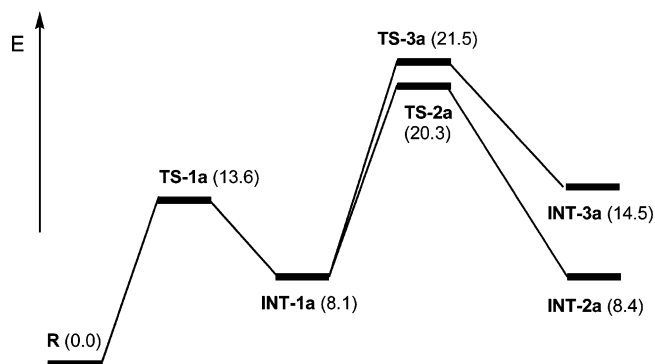


Figure 4. Energy (kcal/mol) profile for the partial and total dissociation of the alkyne from one cobalt center in model complex **R**. Profile corresponds to elongation of bond (a) in **R**.

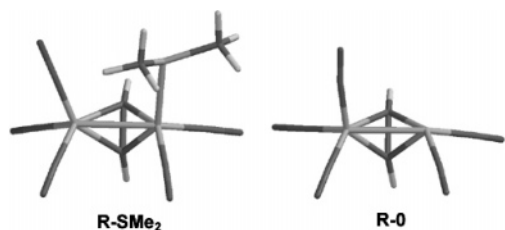


Figure 5. Model structures of dimethylsulfide dicobalt-acetylene complex (**R-SMe₂**) and the same complex without the sulfide ligand and a vacant coordination site (**R-0**).

for the isomerization of the initial tetrahedral dicobalt-alkyne cluster **R**. As shown in Figure 4, the most energetically demanding step is associated with either ligand inversion at the cobalt center (**TS-2a**) or the full dissociation of the alkyne from one of the cobalt atoms (**TS-3a**). In this regard, both reaction pathways are viable from the common butterfly-like intermediate **INT-1a** since they exhibit similar energy requirements. Pseudosymmetric reaction pathways resulting from enlargement of bonds (a) and (b) are almost degenerate (Table 2). Reaction pathway (b) provides a slightly lower energy barrier for the formation of the first intermediate, while in the metal inversion step **TS-2**, path (a), provides a lower energy barrier. The present theoretical model (Figure 4) indicates that the isomerization of P,S-bridged (μ -alkyne) $\text{Co}_2(\text{CO})_4$ complexes through partial or total dissociation of the alkyne from one metal center is a kinetically feasible process under the experimental reaction conditions tested here, i.e., extended heating (60–70 °C) in toluene solution in the absence of CO.

The departure of the sulfide ligand leaving a vacant coordination site on cobalt was also examined computationally. To this end, the DFT (single point) ΔH°_f for model **R-SMe₂** (Figure 5), the corresponding complex **R-0** with a vacant coordination site, and dimethylsulfide were calculated. This provided a theoretical $\Delta H^\circ_f = 15.4$ kcal/mol for the departure of SMe_2 in **R-SMe₂**. An analogous energy barrier should be associated with the cleavage of the Co–S bond in a P,S-bridged complex to yield a vacant coordination site. At this point, migration of the loose phosphine ligand may provide an energetically advantageous isomerization pathway. Taking into account the previously calculated alkyne-dissociation pathway, the present theoretical study suggests that in the absence of CO a complex containing a hemilabile ligand isomerizes through the sulfide-dissociation/phosphine-migration mechanism to preferentially provide the diastereomeric complex in which the C–H \cdots O interaction occurs. The alternative alkyne-dissociation mechanism cannot be completely ruled out; however, this mechanism is more prob-

able for substrates bearing stronger binding ligands (i.e., diphosphines) in which partial dissociation of the ligand is unlikely.¹⁸

Conclusions

The methine moiety contained in PuPHOS and CamPHOS acts as a general nonclassical hydrogen bond donor. Intermolecular contact between this methine and a sulfone hydrogen bond acceptor provides a stabilizing interaction that leads to a diastereoselective coordination of the P,S ligands to a dicobalthexacarbonyl tosylacetylene complex. The diastereoselectivities observed in the ligand exchange process, the X-ray analysis of major diastereomer **2a**, and the quantum mechanical calculations on a model structure indicate that the present C–H \cdots O=S(O)R interaction is slightly less effective than the reported C–H \cdots O=CNR₂. This observation could be attributed to the lower competence of the sulfone moiety to act as a hydrogen bond acceptor in comparison with an amidocarbonyl group. These results validate the generality and efficiency of the present approach as an alternative to steric repulsion for substrate–ligand recognition in asymmetric synthesis and catalysis. Finally, here we have performed a theoretical modeling of the isomerization of P,S-bridged alkyne dicobaltcarbonyl complexes in the absence of CO. Our studies indicate that isomerization for P,S hemilabile ligands occurs via a sulfide-dissociation/phosphine-migration mechanism.

Experimental Section

Dicobalthexacarbonyl Complex of *p*-Tolylsulfonylthyne, **1**.

Solid dicobaltoctacarbonyl (1.42 g, 4.10 mmol) was added to a solution of *p*-tolylsulfonyltrimethylsilylthyne (1.0 g, 3.96 mmol) in diethyl ether (40 mL) under nitrogen. The reaction mixture was stirred at room temperature until CO evolution ceased. The solvent was removed in vacuo, and the resulting red residue was solved in MeOH (120 mL). A $\text{KHCO}_3/\text{K}_2\text{CO}_3$ aqueous buffer solution (6.2×10^{-3} M, 25 mL) was added, and the resulting mixture was stirred at 40 °C for 24 h until no intermediate complex could be detected by TLC. At this stage, 40 mL of water was added and the reaction mixture was filtered over a pad of silica gel. The product complex was then eluted with CH_2Cl_2 . The organic phase was dried (MgSO_4), and the solvent was removed in vacuo to yield 1.5 g (81%) of **1** as an orange crystalline solid. Mp: 155–165 °C (dec). IR (KBr): ν_{max} 2020, 2033, 2053, 2064, 2083, 2107 cm^{-1} . ¹H NMR (300 MHz, CDCl_3): δ 2.43 (s, 3H), 6.24 (s, 1H), 7.34–7.87 (dd, $J = 8$ Hz, 4H) ppm. ¹³C NMR (75 MHz, CDCl_3): δ 21.6, 73.0, 93.3, 127.7, 129.7, 138.1, 144.7, 196.6 (broad, 6CO) ppm. Anal. Calcd for $\text{C}_{15}\text{H}_8\text{Co}_2\text{O}_3\text{S}$: C 38.65, H 1.73, S 6.88. Found: C 38.99, H 1.95, S 6.87.

$\text{Co}_2(\mu\text{-}p\text{-CH}_3\text{-C}_6\text{H}_4\text{C}_2\text{H})(\text{CO})_4(\mu\text{-C}_{23}\text{H}_{27}\text{OPS})$ **1a** and **1b**. A 100 mg (0.21 mmol) portion of dicobalthexacarbonyl complex of *p*-tolylsulfonylthyne, **1**, 80 mg (0.20 mmol) of CamPHOS–borane complex, and 35 mg (0.3 mmol) of DABCO were placed in a Schlenk flask under an argon atmosphere. Then 4 mL of freshly distilled toluene was added, and the mixture was heated at 65 °C. CO was periodically removed from the reaction by means of vacuum and argon refilling. After 16 h, the solvent was removed under reduced pressure. Chromatography (80:20 hexanes/EtOAc) provided 135 mg (85%) of the major (less polar) complex and 18 mg of the minor (more polar) complex as red solids. Data for major complex **1a**: IR (KBr) ν_{max} 2955, 2044, 2018, 1990 cm^{-1} . ¹H NMR (400 MHz, C_6D_6): δ 0.48 (s, 3H), 0.60 (m, 1H), 0.73 (m, 1H), 0.81 (s, 3H), 0.91 (m, 1H), 1.20–1.40 (m, 3H), 1.58 (m, 1H), 1.87 (s, 3H), 2.92 (dd, $J = 6, 13$ Hz, 1H), 3.63 (d, $J = 13$ Hz, 1H), 3.89 (m, 1H), 5.70 (m, 1H), 6.81 (d, $J = 8$ Hz, 1H), 7.04 (s, 1H), 7.05–7.25 (m, 6H), 7.74 (m, 2H), 7.86 (m, 2H), 7.92 (d, $J = 8$ Hz, 2H) ppm. ¹³C NMR (100 MHz, C_6D_6): δ 20.0, 21.2, 22.6, 27.0, 33.7, 37.2, 40.3 ($J = 10$ Hz), 44.8, 45.9, 46.7, 80.0 ($J = 16$ Hz), 87.6 (J

= 3 Hz), 91.3 ($J = 29$ Hz), 128.9 ($J = 10$ Hz), 129.6, 129.9, 130.3, 131.2 ($J = 2$ Hz), 132.2 ($J = 11$ Hz), 134.6, 135.1 ($J = 13$ Hz), 141.2, 143.1 ppm. ^{31}P NMR (121 MHz, C_6D_6): δ 52.8 ppm. MS (FAB-NBA): 764 ($[\text{M} - \text{CO}]^+$, 5%), 736 ($[\text{M} - 2\text{CO}]^+$, 12%), 708 ($[\text{M} - 3\text{CO}]^+$, 24%), 680 ($[\text{M} - 4\text{CO}]^+$, 100%). HRMS: calcd for $\text{C}_{32}\text{H}_{36}\text{Co}_2\text{O}_3\text{PS}_2$ [$\text{M} - 4\text{CO} + \text{H}]^+$, 681.0507, found 681.0508. Data for minor complex **1b**: IR (KBr) ν_{max} 2925, 2042, 2018, 1987 cm^{-1} . ^1H NMR (400 MHz, C_6D_6): δ 0.40–2.00 (m, 7H), 0.66 (s, 3H), 1.30 (s, 3H), 1.91 (s, 3H), 3.02 (m, 1H), 3.50 (m, 1H), 5.40 (s, 1H), 6.34 (s, 1H), 6.90–6.20 (m, 8H), 4.73 (m, 2H), 7.78 (m, 2H), 8.26 (d, $J = 7$ Hz, 2H) ppm. ^{13}C NMR (100 MHz, C_6D_6): δ 20.0, 21.2, 22.4, 27.0, 33.7, 37.0, 41.2, 44.6, 45.8, 46.7, 73.2, 87.3, 90.9 ($J = 24$ Hz), 129.1 ($J = 10$ Hz), 129.6, 130.0, 130.3, 121.0, 131.1 ($J = 11$ Hz), 134.6, 125.8 ($J = 13$ Hz), 140.8, 143.2 ppm. ^{31}P NMR (121 MHz, C_6D_6): δ 55.6 ppm.

$\text{Co}_2(\mu$ -*p*- CH_3 - $\text{C}_6\text{H}_4\text{C}_2\text{H})(\text{CO})_4(\mu$ - $\text{C}_{23}\text{H}_{29}\text{OPS})$ **2a and **2b**.** A 61 mg (0.13 mmol) sample of dicobalthexacarbonyl complex of *p*-tolylsulfonylethyne **1**, 50 mg (0.12 mmol) of PuPHOS–borane complex, and 26 mg (0.24 mmol) of DABCO were placed in a Schlenk flask under an argon atmosphere. Then 2 mL of freshly distilled toluene was added, and the mixture was heated at 65 °C. CO was periodically removed from the reaction by means of vacuum and argon refilling. After 16 h, the solvent was removed under reduced pressure. Chromatography (80:20 hexanes/EtOAc) provided 82 mg (85%) of the major (less polar) complex and 7 mg (7%) of the minor (more polar) complex as red solids. Data for major complex **2a**: IR (KBr): ν_{max} 2045, 2014, 1993, 1968 cm^{-1} . ^1H NMR (300 MHz, C_6D_6): δ 0.22–0.40 (m, 2H), 0.64 (d, $J = 6$ Hz, 3H), 0.68–0.98 (m, 2H), 0.98 (s, 3H), 1.08–1.40 (m, 3H), 1.55–1.74 (m, 1H), 1.65 (s, 3H), 1.87 (s, 3H), 3.43 (m, 1H), 5.86 (s, 1H), 6.80 (d, $J = 8$ Hz, 2H), 6.90 (s, 1H), 7.00–7.32 (m, overlap

with C_6D_6 , 7H), 7.78–7.94 (m, 5H) ppm. ^{13}C NMR (75 MHz, C_6D_6): δ 19.7, 21.2, 21.8, 24.9, 27.4, 30.8, 34.2, 41.0, 49.9 ($J = 8$ Hz), 50.6, 79.0, 81.3, 86.0, 128.2 (overlap with C_6D_6), 128.7 ($J = 9$ Hz), 129.4, 130.0, 130.8, 131.3 ($J = 36$ Hz), 132.9 ($J = 11$ Hz), 134.4, 135.0 ($J = 12$ Hz), 141.2, 142.9 ppm. ^{31}P NMR (121 MHz, C_6D_6): δ –30.6 ppm. HRMS: calcd for $\text{C}_{33}\text{H}_{38}\text{Co}_2\text{O}_4\text{PS}_2$ [$\text{M} - 3\text{CO}]^+$, 711.0613, found 711.0622. Data for minor complex **2b**: IR (KBr): ν_{max} 2043, 2014, 1987, 1968 cm^{-1} . ^1H NMR (300 MHz, C_6D_6): δ 0.22–0.30 (m, 2H), 0.65 (s, 3H), 0.68–0.98 (m, 2H), 0.87 (s, 3H), 0.97 (s, 3H), 1.18–1.22 (m, 3H), 1.55–1.74 (m, 1H), 1.91 (s, 3H), 2.89 (m, 1H), 5.21 (s, 1H), 5.86 (m, 1H), 6.92 (d, $J = 8$ Hz, 2H), 6.90–7.32 (m, overlap with C_6D_6 , 6H), 7.56 (m, 2H), 7.88 (m, 2H), 8.26 (d, $J = 6$ Hz, 2H) ppm. ^{31}P NMR (121 MHz, C_6D_6): δ –28.3 ppm.

Acknowledgment. This work was supported by MEC (CTQ2005-623). X.V. thanks the DURSI for a “Distinció per a la Promoció de la Recerca Universitària”. J.S. thanks the DURSI and Universitat de Barcelona for a fellowship. We thank S. Olivella for helpful advice on quantum mechanics calculations.

Supporting Information Available: General methods; ^1H NMR spectra for major complexes **1a** and **2a**; X-ray crystal data with a complete numbering scheme, atomic distances and angles for **2a**; computing model for hydrogen bond contact and complete ref 19; Cartesian coordinates for molecular modeling compounds and transition states. This material is available free of charge via the Internet at <http://pubs.acs.org>.

OM060656M